Erratum: $\Lambda_b \to J/\psi K\Xi$ decay and the higher order chiral terms of the meson baryon interaction [Phys. Rev. D 92, 076015 (2015)]

A. Feijoo, V. K. Magas, A. Ramos, and E. Oset
(Received 31 January 2017; published 22 February 2017)

There should be a change of sign in the coefficients of the $\eta(\eta')\Lambda$ components in the hadronized state, such that Eq. (1) in the original paper changes to

$$|H\rangle = |K^- p\rangle + |\bar{K}^0 n\rangle + \frac{\sqrt{2}}{3}|\eta\Lambda\rangle - \frac{2}{3}|\eta'\Lambda\rangle. \tag{1}$$

This modification is tied to a change of sign in the Λ wave function, which is needed for consistency with the sign conventions of the chiral meson-baryon Lagrangian [1]. As a consequence, the weight $h_{\eta\Lambda}$ employed throughout the paper becomes $h_{\eta\Lambda} = \sqrt{2}/3$.[1]

This change affects the value of the matrix element for the decay of the Λ_b into a J/Ψ and a meson-baryon pair $(\phi_j B_j)$, reproduced here for the sake of facilitating the discussion,

$$\mathcal{M}_j(M_{\text{inv}}) = V_p\left(h_j + \sum_i h_i G_i(M_{\text{inv}})t_{ij}(M_{\text{inv}})\right), \tag{2}$$

where G_i denotes the one-meson–one-baryon loop function, chosen in accordance with the model for the scattering amplitude t_{ij} describing the strangeness $S = -1$ meson-baryon interaction. The coefficients needed to connect to the isospin $I = 0$ term of this interaction, the only component acting on the decay of the Λ_b, are

$$h_{\pi^0\Sigma^0} = h_{\pi^+\Sigma^-} = h_{\pi^-\Sigma^+} = 0, \qquad h_{\eta\Lambda} = \frac{\sqrt{2}}{3}, \tag{3}$$

$$h_{K^- p} = h_{\bar{K}^0 n} = 1, \qquad h_{K^+\Xi^-} = h_{K^0\Xi^0} = 0. \tag{4}$$

It is then obvious that a new pattern of interferences emerges with the change of sign of the $h_{\eta\Lambda}$ coefficient, and Figs. 4 to 7 in the original manuscript must be replaced by the ones shown below.

The invariant mass distributions of $\pi\Sigma$ states in Fig. 4 show a minimum located essentially where there was a maximum before. The process leading to a final $J/\psi\pi\Sigma$ state lacks a tree-level term; hence, the changes just reflect the transition from a constructive to a destructive interference between the $\eta\Lambda$ and $\bar{K}N$ contributions present in the rescattering term of Eq. (2). The qualitative changes in the invariant mass distributions of $\bar{K}N$ states are less pronounced, since the $\Lambda_b \to J/\Psi\bar{K}N$ decay also receives contributions from the featureless tree-level term and, in addition, the $\bar{K}N \to \bar{K}N$ amplitude is dominant over the $\eta\Lambda \to \bar{K}N$ one in the rescattering term. The new $\pi\Sigma$ to $\bar{K}N$ distributions also lead to a modified ratio at their respective maximum values, established to be 4.9 and 3.5 for models 1 and 2, respectively, in the original paper. Now, this ratio amounts to a value of around 3 for model 1 (dashed lines), while it cannot be established for model 2 (solid lines), since the $\bar{K}N$ distribution does not present a maximum in the explored range of energies.

The invariant mass distributions of $K^+\Xi^-$ states of the new Fig. 5 present a strength reduced by a factor of about 10 with respect to the ones of the original manuscript. This is due to a destructive interference between $\eta\Lambda \to K\Xi$ and $\bar{K}N \to K\Xi$ amplitudes present in the rescattering term, since the tree-level contribution is absent in the $\Lambda_b \to J/\psi K^+\Xi^-$ decay process. However, the shapes of the distributions present similar qualitative features, and the discussion in the original paper remains valid.

---

[1]One should also modify the $\eta'\Lambda$ weight to $h_{\eta'\Lambda} = -2/3$, but this change does not affect the results because the $\eta'\Lambda$ component was neglected in the original paper.
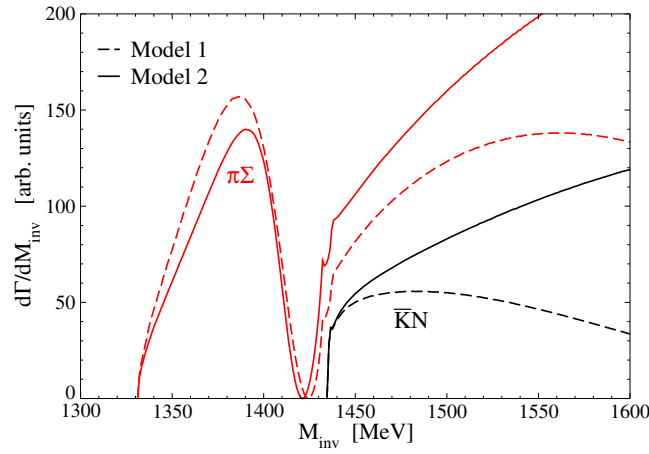
039905-1

FIG. 4. Invariant mass distributions of $\pi\Sigma$ and $\bar{K}N$ states in the decay modes $\Lambda_b \to J/\psi\pi\Sigma$ and $\Lambda_b \to J/\psi\bar{K}N$, for the two models discussed in the text: model 1 (dashed lines) and model 2 (solid lines). The units in the y axis are obtained taking $V_p = 1$.
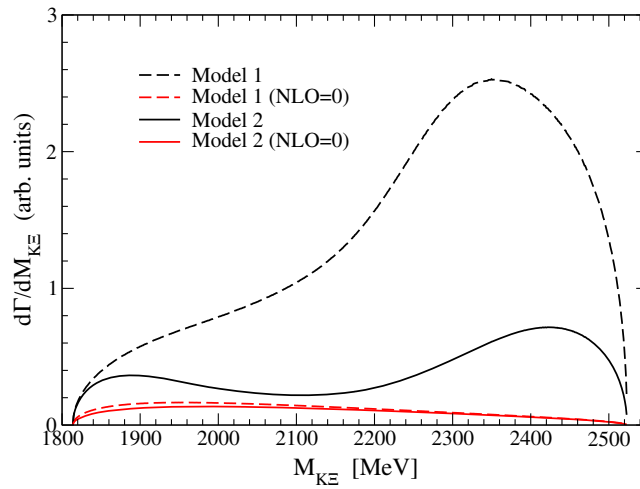

FIG. 5. Invariant mass distributions of $K^+\Xi^-$ states produced in the decay $\Lambda_b \to J/\psi K^+\Xi^-$, obtained for the two models discussed in the text: model 1 (dashed lines) and model 2 (solid lines). The thin lower lines correspond to omitting the next-to-leading-order (NLO) terms of the potential. The normalization is the same as in Fig. 4.
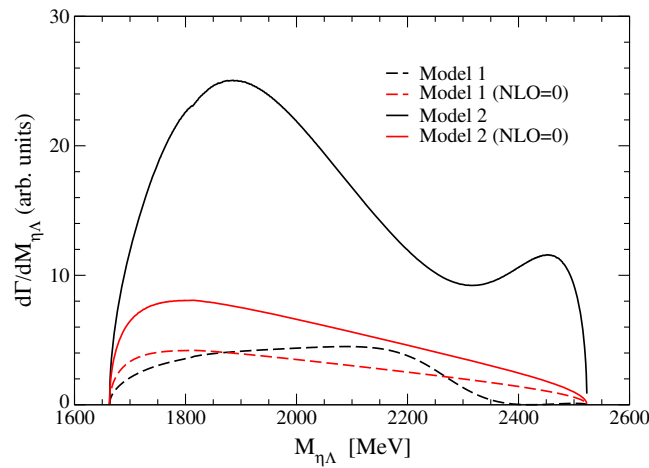

FIG. 6. Invariant mass distributions of $\eta\Lambda$ states produced in the decay $\Lambda_b \to J/\psi\eta\Lambda$, obtained for the two models discussed in the text: model 1 (dashed lines) and model 2 (solid lines). The thin lower lines correspond to omitting the NLO terms of the potential. The normalization is the same as in Fig. 4.
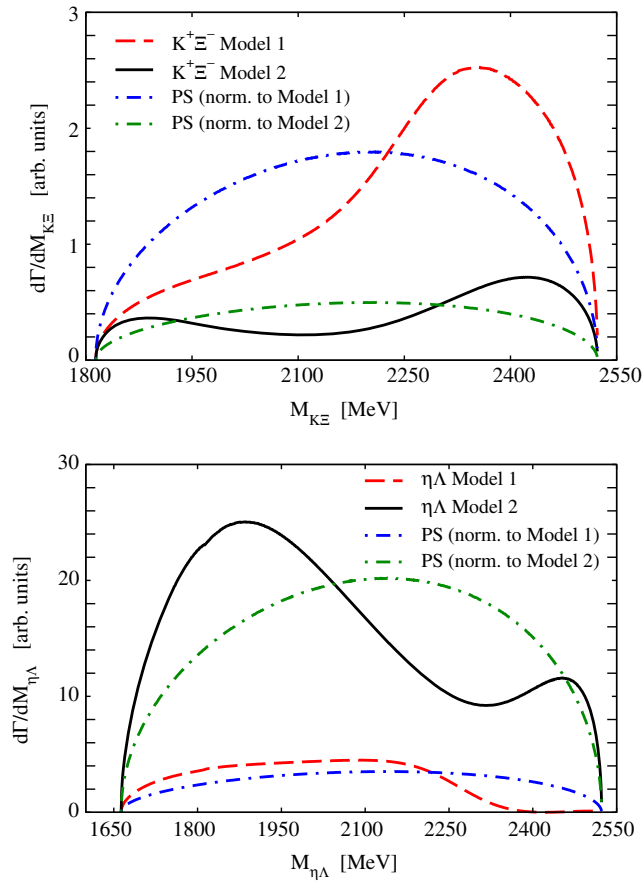
FIG. 7.   Comparison of the invariant mass distributions of $K^+\Xi^-$ states (upper panel) and $\eta\Lambda$ states (lower panel) obtained with model 1 (dashed lines) and model 2 (solid lines) with a pure phase-space distribution (dotted lines).

The $\eta\Lambda$ invariant mass spectra shown in the new Fig. 6 are substantially affected by the change of sign of $h_{\eta\Lambda}$, both in size and shape. There is now a destructive interference between the featureless tree-level contribution and the rescattering term, such that the new distributions show a fall or a dip in the energy region around 2300 MeV where the original ones presented a maximum. In the case of model 1 (dashed lines), since the contribution of the tree-level term turns out to be very similar in size to that of the rescattering term, the strength of the resulting distribution is substantially reduced compared to that in the original paper. As a consequence, the magnitude of the $\Lambda_b \to J/\psi\eta\Lambda$ distribution for model 1 is of the same order as the $\Lambda_b \to J/\psi K\Xi$ one, even if the latter does not receive the contribution from a tree-level term. In the case of model 2 (solid lines), the $\Lambda_b \to J/\psi\eta\Lambda$ distribution is on average 30 times larger than the $\Lambda_b \to J/\psi K\Xi$ one.

Finally, the invariant mass distributions from the $\Lambda_b \to J/\psi K^+\Xi^-$ and $\Lambda_b \to J/\psi\eta\Lambda$ decays obtained in models 1 and 2 are compared with the phase space in the new Fig. 7. The dynamical features of the meson-baryon amplitudes lead to distinct shapes of the mass distributions compared to phase space. In the case of model 1 (dashed line), we observe a peaked structure around 2300 MeV in the $K^+\Xi^-$ distribution, as in the original paper, and a sharp fall starting at 2250 MeV for the $\eta\Lambda$ one, contrary to the peak seen in the original paper. Similar behavior is found in the case of model 2 (solid lines), although the peak in the $K^+\Xi^-$ invariant mass spectrum is slightly shifted to a higher energy, and the fall becomes a dip in the $\eta\Lambda$ one.

In spite of these changes, the conclusions of the paper remain the same, emphasizing the role of the $\Lambda_b \to J/\psi K^+\Xi^-$ and $\Lambda_b \to J/\psi\eta\Lambda$ decays as processes that can provide valuable information on the meson-baryon interaction in the strangeness $S = -1$ sector.

[1] R. P. Pavao, W. H. Liang, J. Nieves, and E. Oset, arXiv:1701.06914.